Supplemental Figures

Figure S1

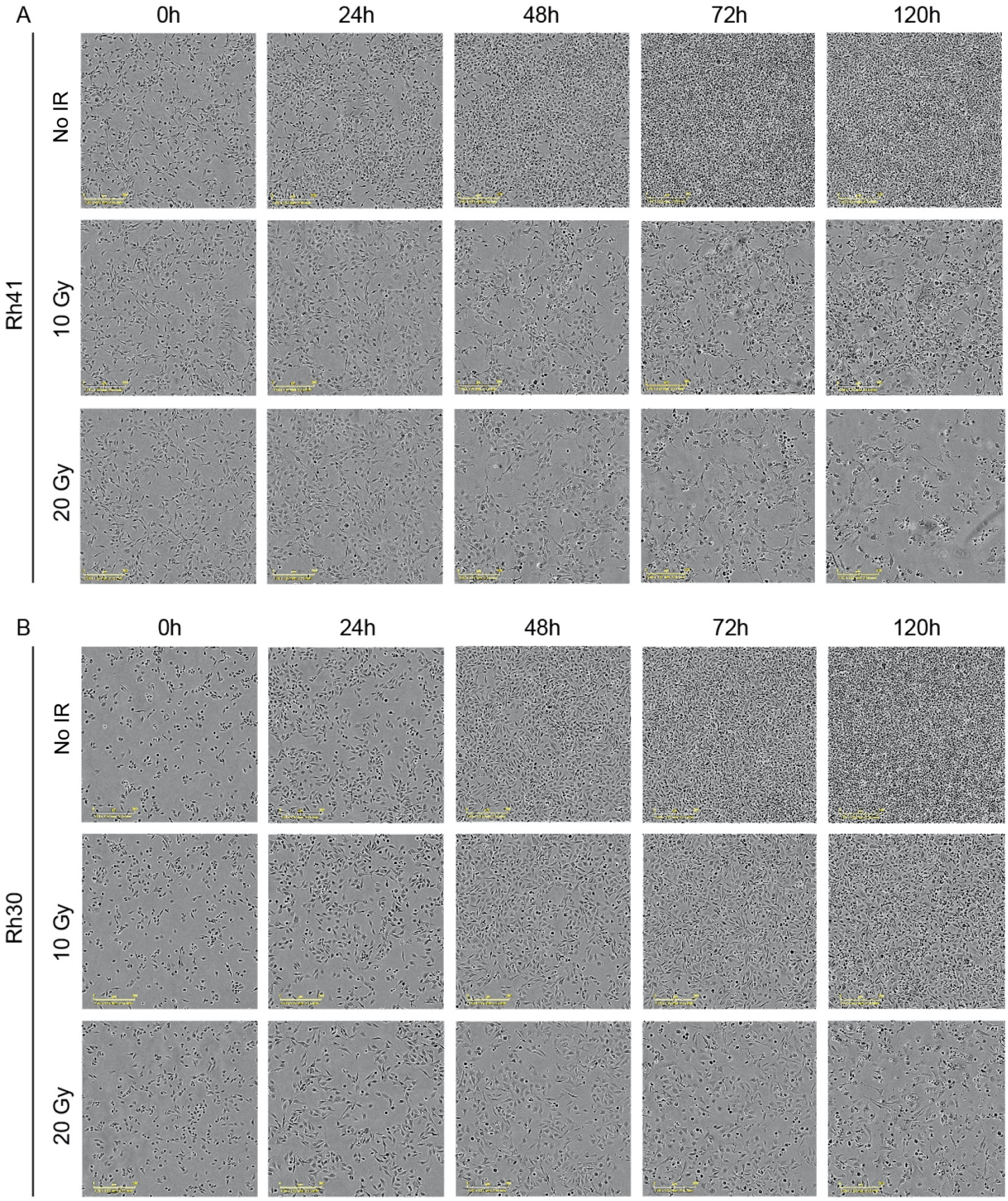

Supplemental Figure 1.

A, B. Examples of Growth of IR sensitive Rh41 and IR resistant Rh30 cells after irradiation with increasing doses of IR at various time points post exposure. Representative images shown. Scale bar 300 μm.

Figure S2

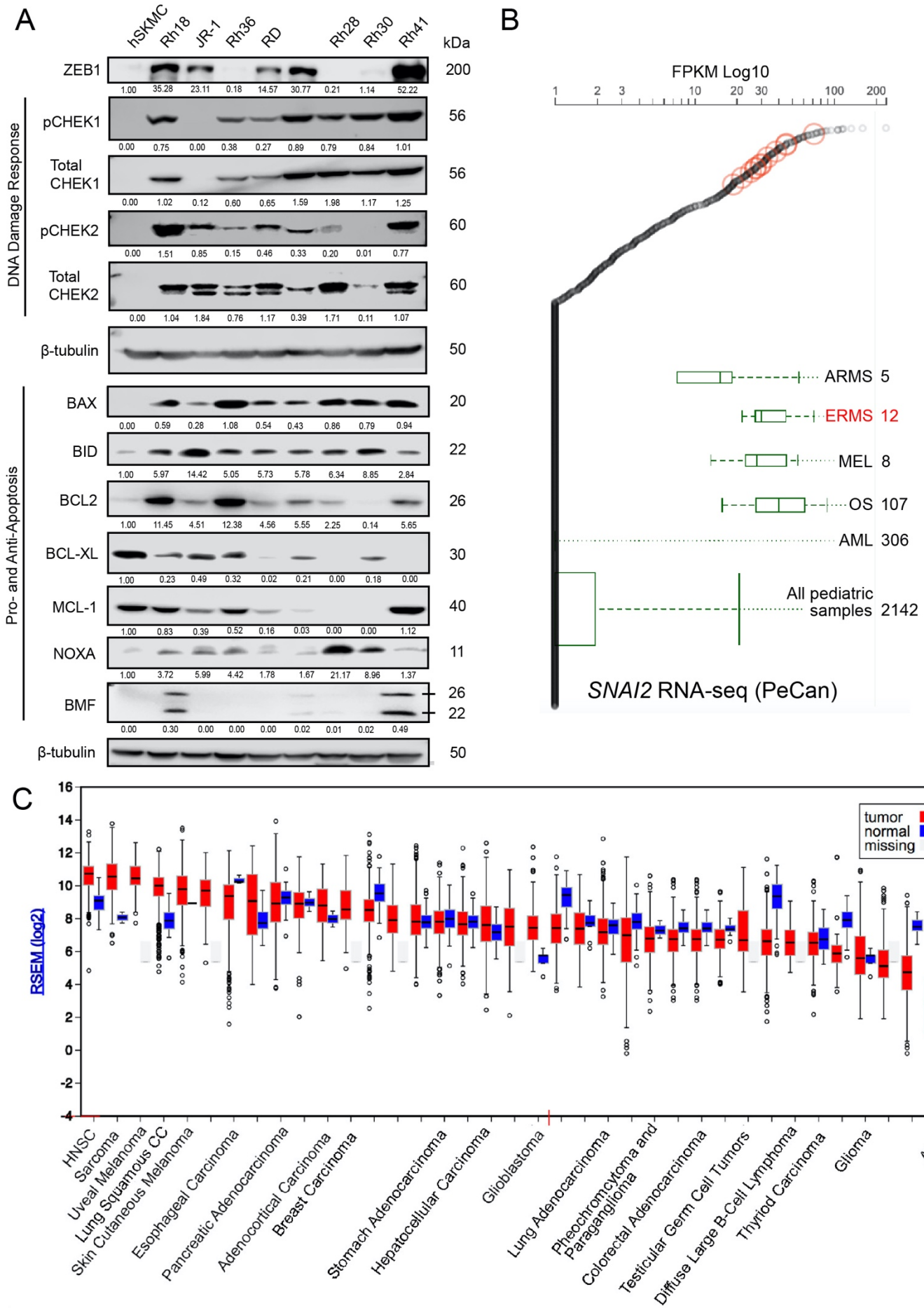
A
hSKMC
Rh18
JR-1
Rh36
RD
Rh28
Rh30
Rh41
kDa
DNA Damage Response
ZEB1
200
1.00 35.28 23.11 0.18 14.57 30.77 0.21 1.14 52.22
pCHEK1
56
0.00 0.75 0.00 0.38 0.27 0.89 0.79 0.84 1.01
Total CHEK1
56
0.00 1.02 0.12 0.60 0.65 1.59 1.98 1.17 1.25
pCHEK2
60
0.00 1.51 0.85 0.15 0.46 0.33 0.20 0.01 0.77
Total CHEK2
60
0.00 1.04 1.84 0.76 1.17 0.39 1.71 0.11 1.07
β-tubulin
50
Pro- and Anti-Apoptosis
BAX
20
0.00 0.59 0.28 1.08 0.54 0.43 0.86 0.79 0.94
BID
22
1.00 5.97 14.42 5.05 5.73 5.78 6.34 8.85 2.84
BCL2
26
1.00 11.45 4.51 12.38 4.56 5.55 2.25 0.14 5.65
BCL-XL
30
1.00 0.23 0.49 0.32 0.02 0.21 0.00 0.18 0.00
MCL-1
40
1.00 0.83 0.39 0.52 0.16 0.03 0.00 0.00 1.12
NOXA
11
1.00 3.72 5.99 4.42 1.78 1.67 21.17 8.96 1.37
BMF
26
22
0.00 0.30 0.00 0.00 0.00 0.02 0.01 0.02 0.49
β-tubulin
50
B
FPKM Log10
1 2 3 10 20 30 100 200
ARMS 5
ERMS 12
MEL 8
OS 107
AML 306
All pediatric samples 2142
SNAI2 RNA-seq (PeCan)
C
RSEM (log2)
16 14 12 10 8 6 4 2 0 -2 -4
tumor
normal
missing
HNSC
Sarcoma
Uveal Melanoma
Lung Squamous CC
Skin Cutaneous Melanoma
Esophageal Carcinoma
Pancreatic Adenocarcinoma
Adenocortical Carcinoma
Breast Carcinoma
Stomach Adenocarcinoma
Hepatocellular Carcinoma
Glioblastoma
Lung Adenocarcinoma
Pheochromocytoma and Paraganglioma
Colorectal Adenocarcinoma
Testicular Germ Cell Tumors
Diffuse Large B-Cell Lymphoma
Thyriod Carcinoma
Glioma
AML

Supplemental Figure 2.

A. Western blots showing levels of ZEB1, DNA damage response proteins, and pro- and anti-apoptotic proteins across rhabdomyosarcoma cell lines; hSKMC, human Skeletal muscle cells were used as control for western blot analyses.

B. *SNAI2* expression in RMS tumors compared to other pediatric cancers, with *SNAI2* expression levels in ERMS tumors circled in red (ARMS – alveolar rhabdomyosarcoma, ERMS – embryonal rhabdomyosarcoma, MEL – melanoma, OS – osteosarcoma, AML – acute myeloid leukemia; St Jude PeCan database)-Note this is the same data from Figure 1F but includes expression of *SNAI2* comparisons to other pediatric cancers.

C. *SNAI2* expression levels in tumors in the TCGA database.

Figure S3

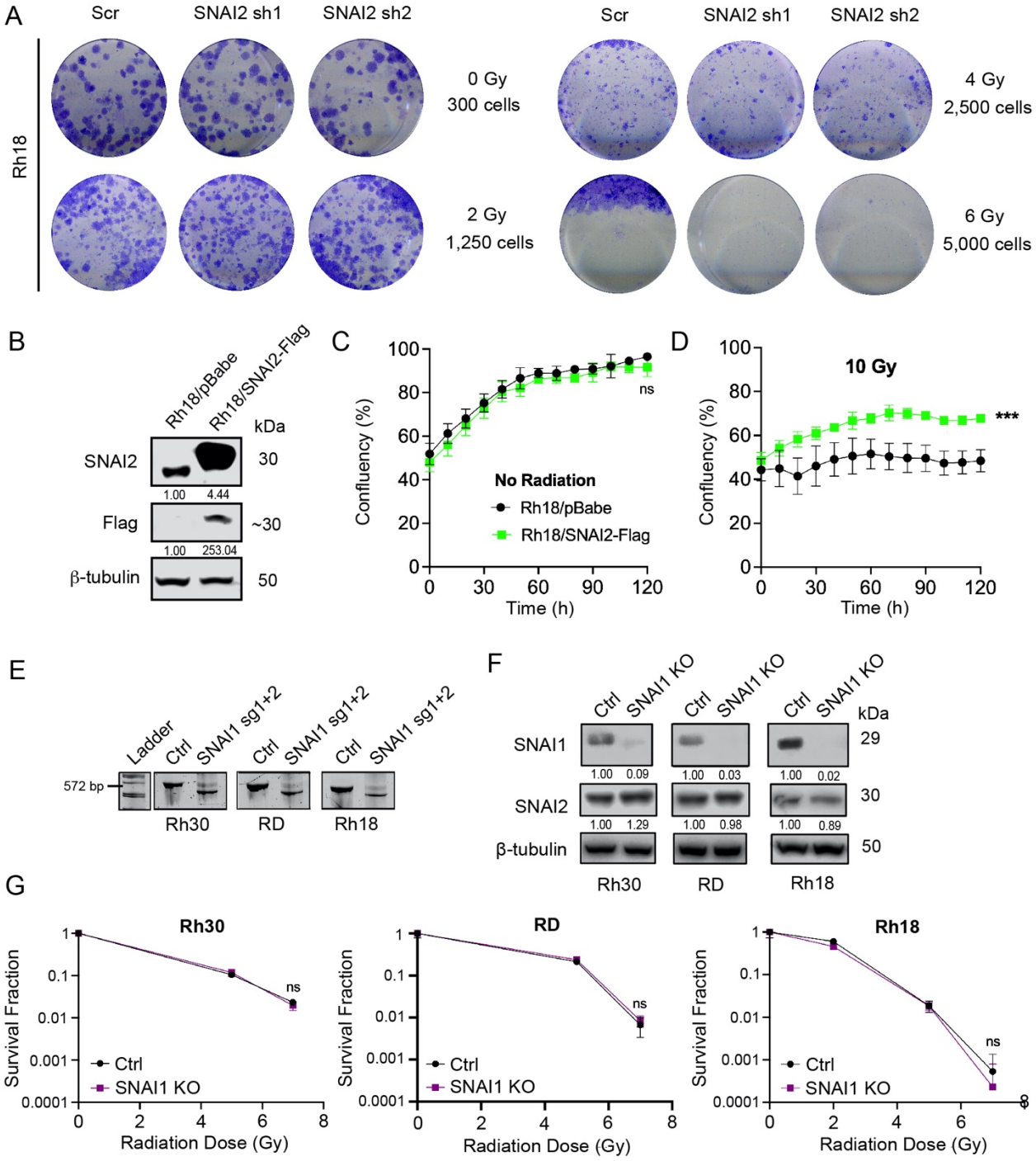

Supplemental Figure 3.

A. Representative colony formation wells for Rh18 Scr and SNAI2 knockdown (sh1 and sh2) after indicated IR exposure.

B. Western blot of Rh18 pBabe control and SNAI2-Flag cells for SNAI2 and Flag expression.

C, D. Confluency (%) of non-IR or IR-treated (10 Gy) Rh18 pBabe or SNAI2-Flag cells was assessed on phase-contrast images acquired from 0 to 130 h. Error bars represent ±1 SD. ns = not significant, ***p<0.001 by two-way ANOVA with Sidak's multiple comparisons test.

E. Deletion of a significant part of coding region of SNAI1 Exon 1 (78-87%) using two CRISPR sgRNA guides (sg1 and sg2) that are analyzed by genomic PCR and 6% polyacrylamide gel electrophoresis (PAGE). In all three cell lines (Rh30, RD and Rh18), control (Ctrl) lanes show a single 572 bp wildtype amplicon while the sg1+2 lanes show a prominent amplicon 70-90 bp smaller than the wildtype amplicon.

F. Western blots of Rh30, RD, and Rh18 Scr and SNAI1 CRISPR KO cells for SNAI1 and SNAI2 expression.

G. Survival fractions of Rh30, RD, and Rh18 Ctrl versus SNAI1 KO cells were assessed at increasing IR dose exposures. Statistical differences were observed at 6 Gy. Error bars represent ±1 SD. ns = not significant by one-way ANOVA with Dunnett's multiple comparisons test.

Figure S4

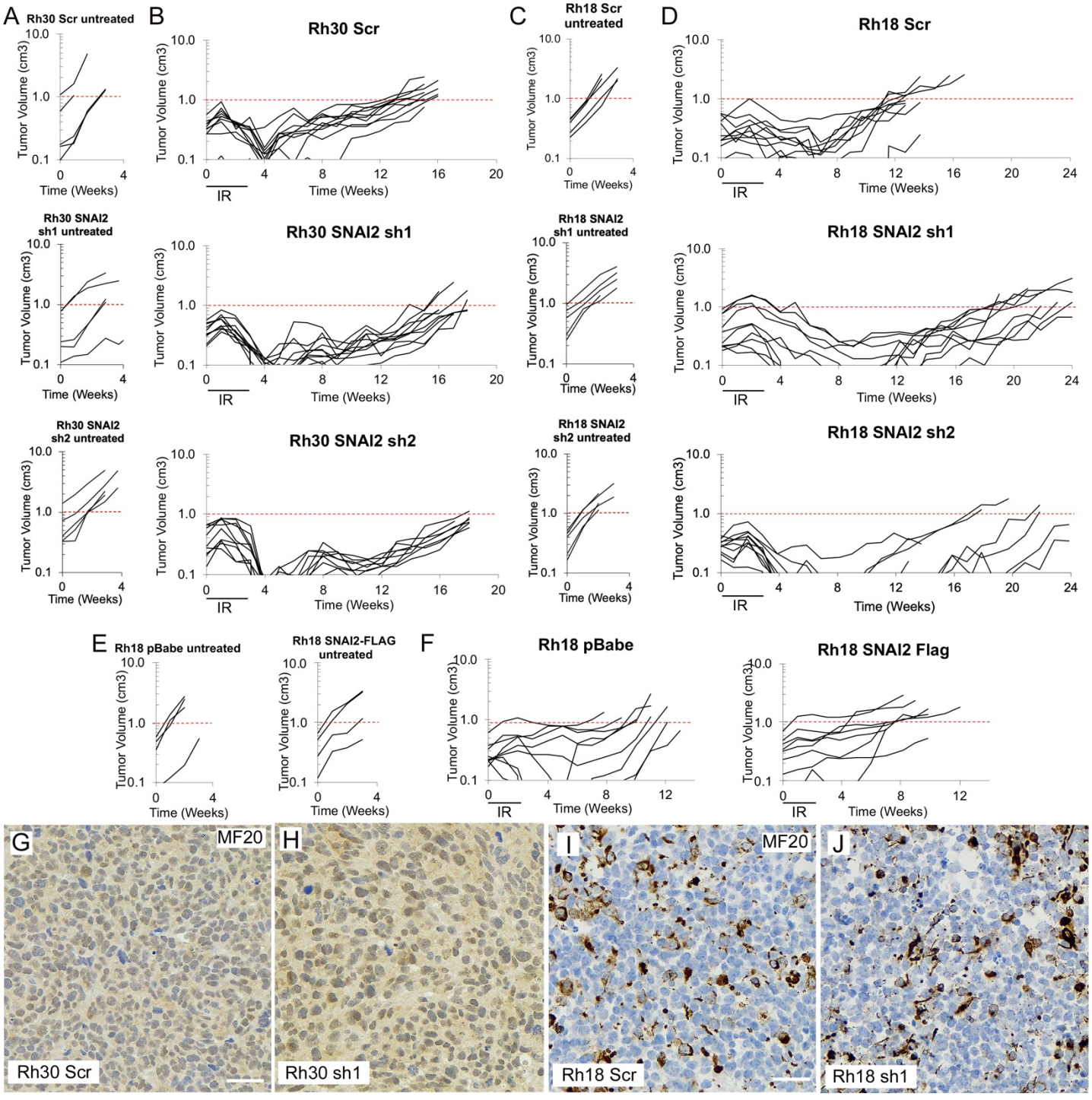

Supplemental Figure 4.

A. Individual tumor volumes for Rh30 Scr, SNAI2 sh1, and SNAI2 sh2 xenografts under non-IR conditions.

B. Individual tumor volumes for Rh30 Scr, SNAI2 sh1, and SNAI2 sh2 xenografts after IR exposure (2 Gy/day, 5x a week, for 3 weeks).

C. Individual tumor volumes for Rh18 Scr, SNAI2 sh1, and SNAI2 sh2 xenografts under non-IR conditions.

D. Individual tumor volumes for Rh18 Scr, SNAI2 sh1, and SNAI2 sh2 xenografts after IR exposure (2 Gy/day, 5x a week, for 3 weeks).

E. Individual tumor volumes for Rh18 pBabe and SNAI2-Flag xenografts under non-IR conditions. Red dashed line indicates 1 cm^3 in all graphs.

F. Individual tumor volumes for Rh18 pBabe and SNAI2-Flag xenografts after IR exposure (2 Gy/day, 5x a week, for 2 weeks).

G, H. Representative immunohistochemistry sections of MyHC (MF20) staining in Rh30 Scr and SNAI2 sh1 xenografts. No statistical difference detected. Scale bar = 100 μm.

I, J. Representative immunohistochemistry sections of MyHC (MF20) staining in Rh18 Scr and SNAI2 sh1 xenografts. No statistical difference detected. Scale bar = 100 μm.

Figure S5

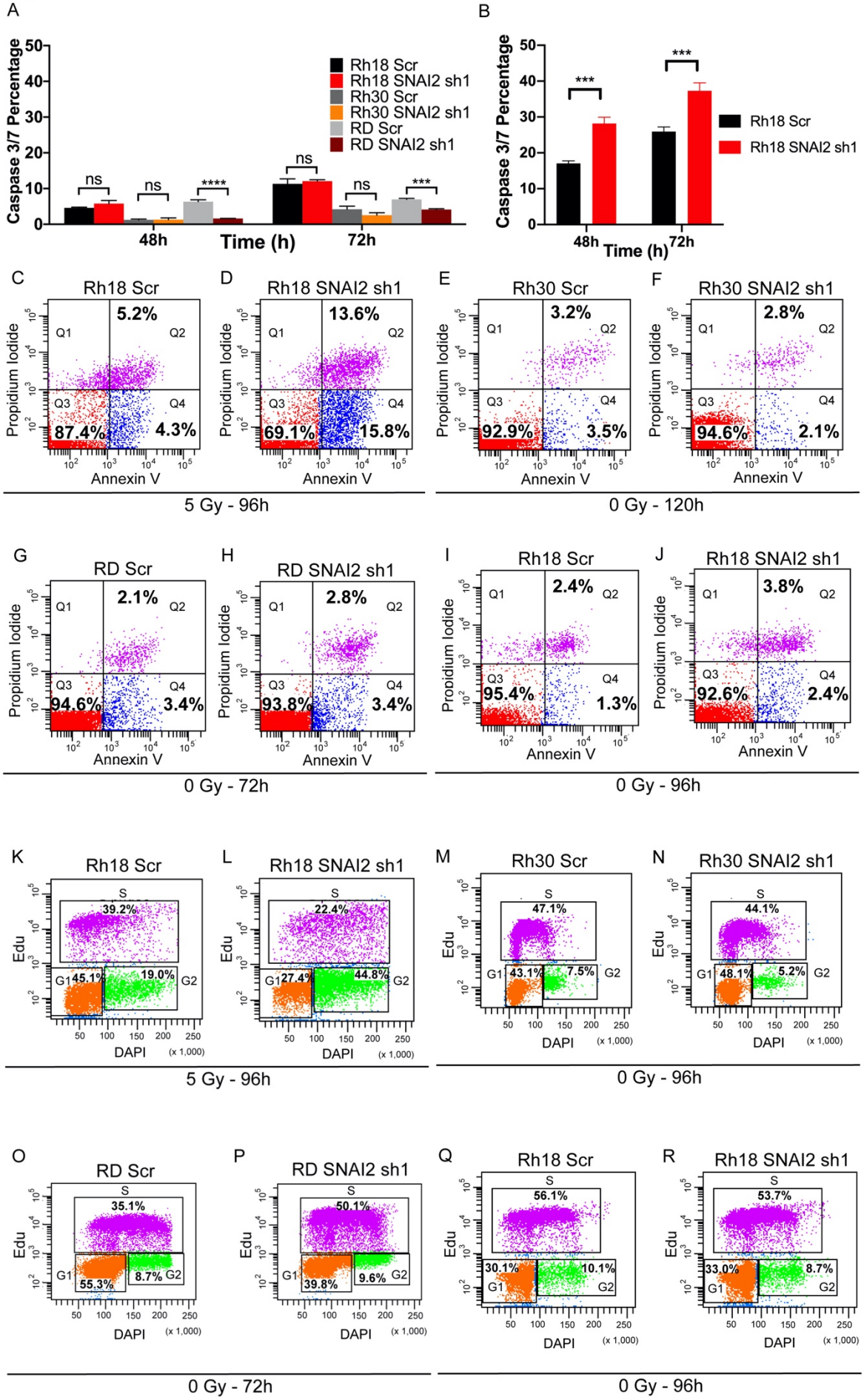
A
Caspase 3/7 Percentage
Rh18 Scr
Rh18 SNAI2 sh1
Rh30 Scr
Rh30 SNAI2 sh1
RD Scr
RD SNAI2 sh1
ns
ns
****
ns
ns
***
48h
Time (h)
72h
B
Caspase 3/7 Percentage
***
***
Rh18 Scr
Rh18 SNAI2 sh1
48h
Time (h)
72h
C
Rh18 Scr
5.2%
87.4%
4.3%
D
Rh18 SNAI2 sh1
13.6%
69.1%
15.8%
E
Rh30 Scr
3.2%
92.9%
3.5%
F
Rh30 SNAI2 sh1
2.8%
94.6%
2.1%
Propidium Iodide
Annexin V
Q1
Q2
Q3
Q4
5 Gy - 96h
0 Gy - 120h
G
RD Scr
2.1%
94.6%
3.4%
H
RD SNAI2 sh1
2.8%
93.8%
3.4%
I
Rh18 Scr
2.4%
95.4%
1.3%
J
Rh18 SNAI2 sh1
3.8%
92.6%
2.4%
0 Gy - 72h
0 Gy - 96h
K
Rh18 Scr
S
39.2%
G1
45.1%
19.0%
G2
L
Rh18 SNAI2 sh1
22.4%
27.4%
44.8%
M
Rh30 Scr
47.1%
43.1%
7.5%
N
Rh30 SNAI2 sh1
44.1%
48.1%
5.2%
Edu
DAPI
(x 1,000)
5 Gy - 96h
0 Gy - 96h
O
RD Scr
35.1%
55.3%
8.7%
P
RD SNAI2 sh1
50.1%
39.8%
9.6%
Q
Rh18 Scr
56.1%
30.1%
10.1%
R
Rh18 SNAI2 sh1
53.7%
33.0%
8.7%
0 Gy - 72h
0 Gy - 96h

Supplemental Figure 5. Related to Figure 4; Loss of SNAI2 promotes IR-mediated apoptosis and blocks irradiated RMS cells from exiting the cell cycle.

A**.** Average Caspase 3/7 percentages (mean ± 1 SD) of Rh18, RD, and Rh30 cells (either Scr shRNA or SNAI2 shRNA) undergoing apoptosis grown under non-IR conditions. ns = not significant, ***p<0.001, ****p<0.0001 by two-way ANOVA with Sidak's multiple comparison.

B. Average Caspase 3/7 percentages (mean ± 1 SD) of Rh18 cells with either Scr shRNA or SNAI2 shRNA undergoing apoptosis after a 5 Gy IR dose. ***p<0.001 by two-way ANOVA with Sidak's multiple comparison.

C, D. Flowcytometry plots showing Propidium iodide vs. Annexin V staining in Rh18 cell lines with either Scr shRNA or SNAI2 shRNA knockdown after treatment with a 5 Gy IR dose. Rh18 early apoptosis (Q4): Scr 4.3% vs. sh1 15.8%, p<0.0001, late apoptosis (Q2): Scr 5.2% vs. sh1 13.6%, p<0.0001 by Two Proportions Z-test.

E-J. Flow cytometry plots showing Propidium iodide vs. Annexin V staining in Rh30, RD, and Rh18 cell lines with either Scr shRNA or SNAI2 shRNA knockdown under growth conditions without IR. Rh30 Scr vs. sh1, Q2 – p=0.60306, Q4 – p=0.05744; RD Scr vs. sh1, Q2 – p=0.3125, Q4 – p=1; Rh18 Scr vs. sh1, Q2 – p=0.0703, Q4 – p=0.06724 by Two Proportions Z-test.

K, L. Flowcytometry plots of EdU vs. DAPI staining in Rh18 cells with either Scr shRNA or SNAI2 sh1 after exposure to 5 Gy. Rh18 vs. sh1 G2 phase p<0.0001 by Two Proportions Z-test.

M-R. Flow cytometry plots showing cell cycle analysis with EdU vs. DAPI staining in Rh18, RD, and Rh30 cells with either Scr shRNA or SNAI2 shRNA under growth conditions without IR. Rh30 Scr vs. sh1, p=0.7062; RD Scr vs. sh1, p=1; Rh18 Scr vs. sh1, p=0.9228 by Two Proportions Z-test.

Figure S6

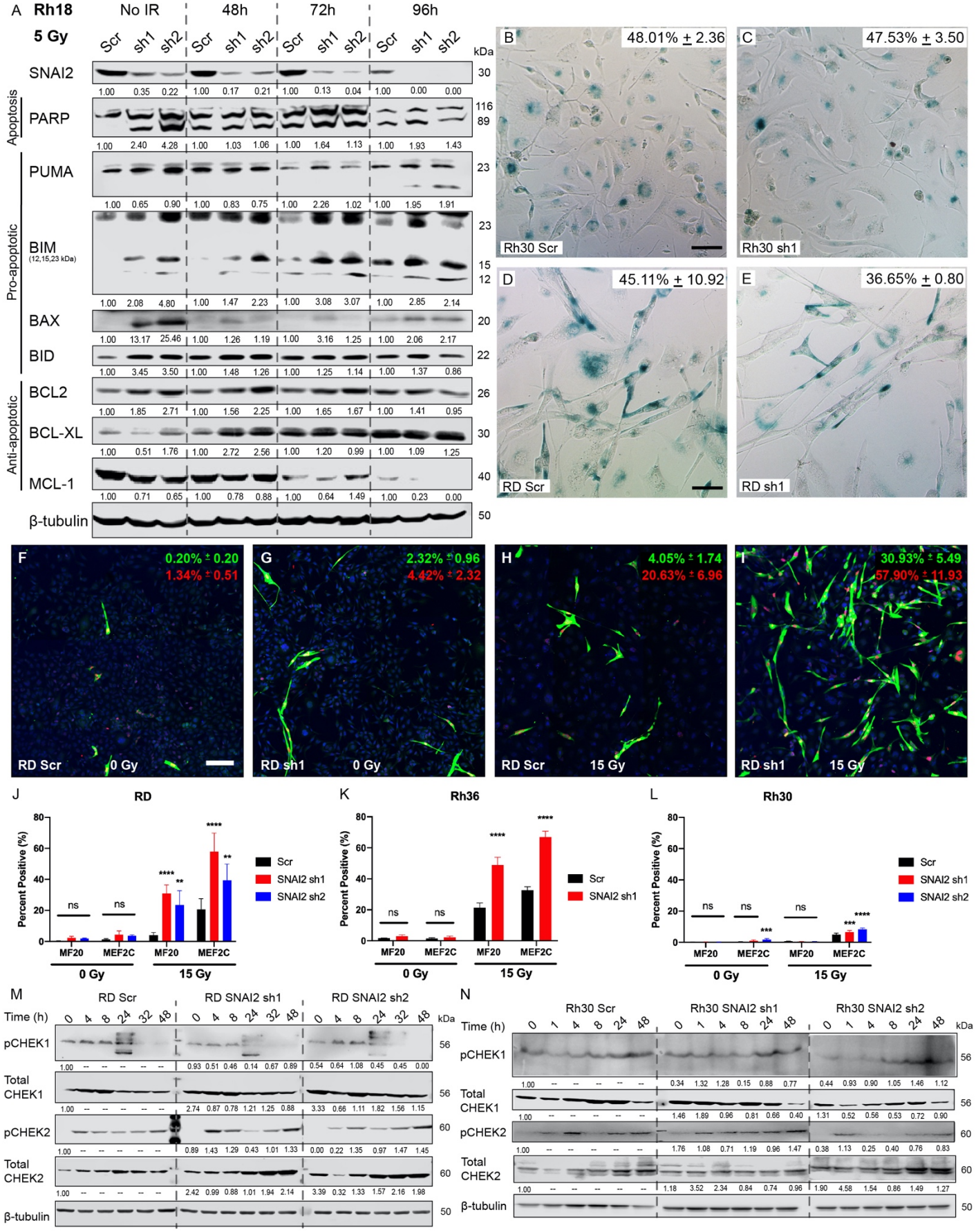

Supplemental Figure 6.

A. Western blot showing levels of apoptotic, pro-apoptotic, and anti-apoptotic proteins in Rh18 cells with control or SNAI2 knockdown, with and without IR and assessed at 48, 72, and 96 hpIR with 5 Gy.

B-E. β-gal staining in Rh30 and RD cells with either Scr shRNA or SNAI2 shRNA treatments at 120h post IR (20 Gy). No statistical difference in percentage of β-gal staining. Scale bar = 5 μm.

F-I. Representative confocal microscopy images of RD cells with either Scr or SNAI2 shRNA expression immunostained with differentiated myosin MF20 and MEF2C antibodies under non-IR (F, G) or 15 Gy (H, I) IR conditions. Scale bar = 100 μm.

J-L. Quantification of average MF20 and MEF2C in either non-IR or 15 Gy IR conditions in Scr vs SNAI2 shRNA treated RD, Rh36, and Rh30 cells. Error bars represent $\pm$1 SD. ns = not significant, **p<0.005, ***p<0.001, ****p<0.0001 by two-way ANOVA with Sidak's multiple comparisons test.

M. Western blots showing expression of phosphorylated CHEK1 and total CHEK1, as well as phosphorylated CHEK2 and total CHEK2, in RD cells with either Scr shRNA or SNAI2 shRNA treatments.

N. Western blot showing levels of phosphorylated CHEK1 and total CHEK1, as well as phosphorylated CHEK2 and total CHEK2, in Rh30 cells with either Scr shRNA or SNAI2 shRNA treatments.

Figure S7

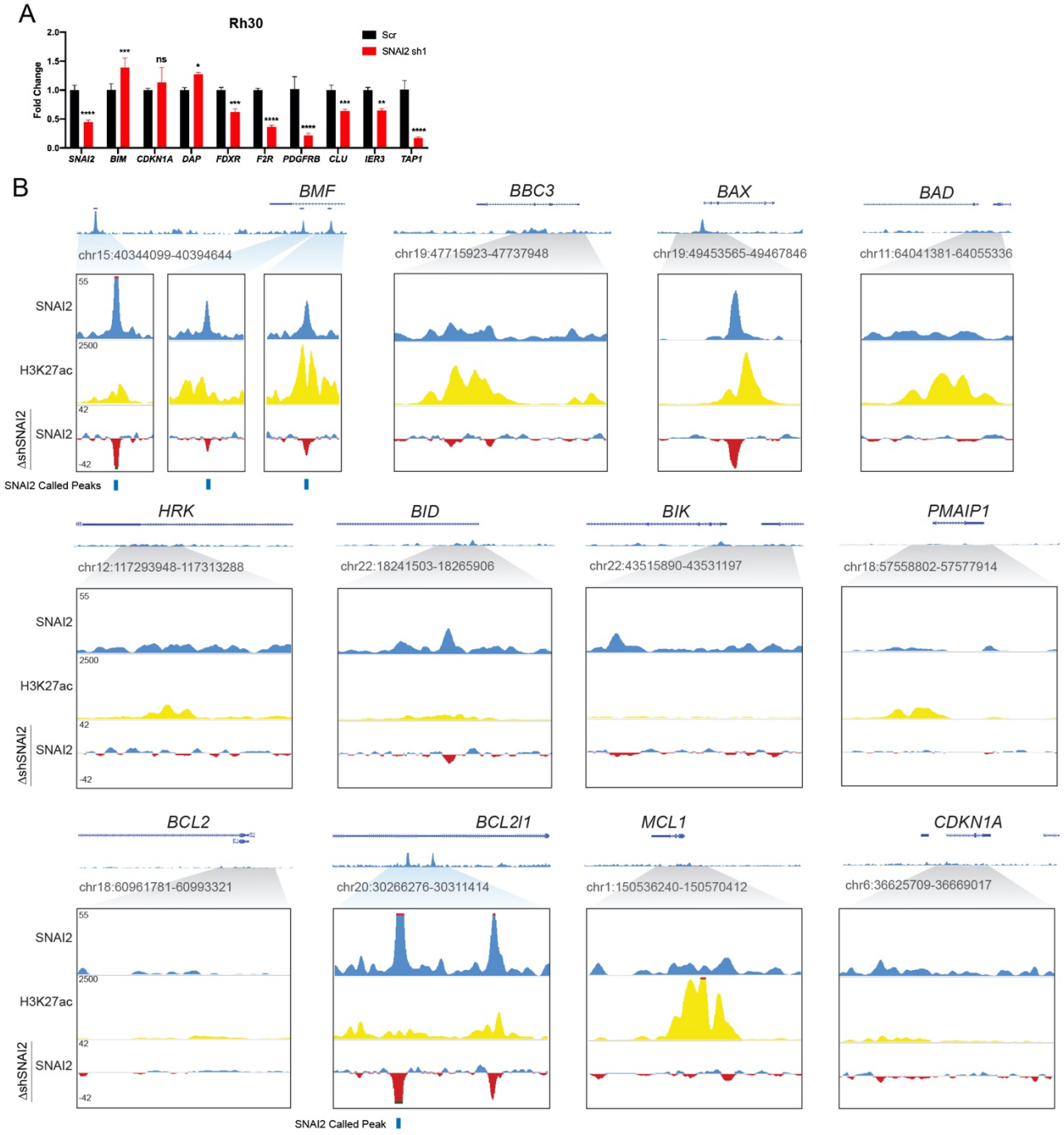

Supplemental Figure 7.

A. Real time qPCR analysis (mean ± 1 SD) of various cell cycle and apoptosis genes in Rh30 cells 48h after irradiation with 10 Gy. ns = not significant, *p<0.05, **p<0.005, ***p<0.001, ****p<0.0001 by two-way ANOVA with a Sidak's multiple comparisons test.

B. ChIP-seq tracks of SNAI2 (Blue) and H3K27ac (Yellow) binding in SMS-CTR cells in shScr cells and delta (Δ) enrichment value (shSNAI2 sh1 minus shScr, Blue and Red) for SNAI2 for *BMF, PUMA/BBC3, BAX, BAD,*

HRK, BID, BIK, NOXA/PMAIP1, BCL2, BCL2L1, MCL1, and *CDKN1A*. Shaded areas denote relative position of SNAI2 binding site to the gene and blue shades are SNAI2 called peaks. Values on Y-axis represent fold enrichment.

Figure S8

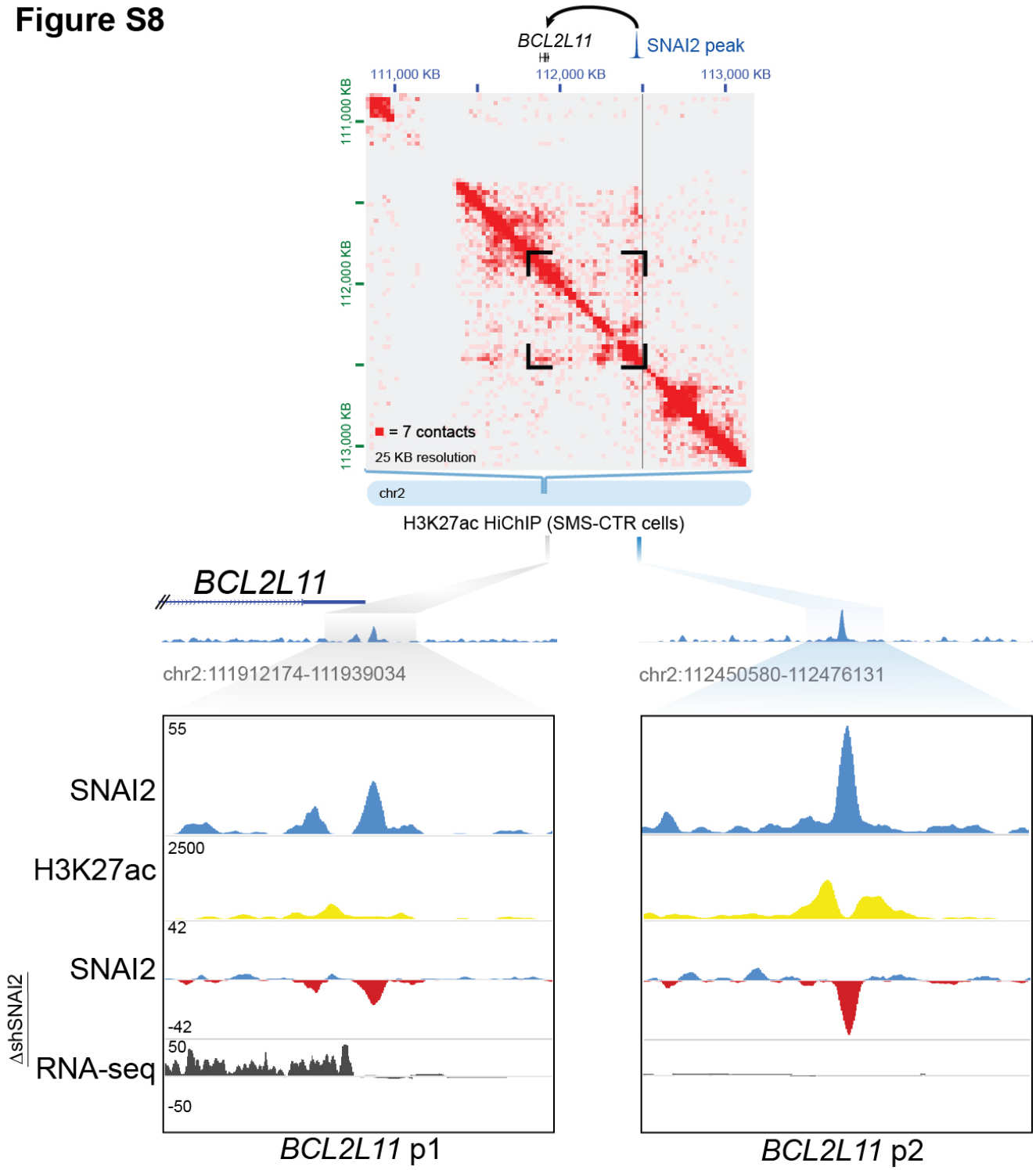

Supplemental Figure 8.

Location of SNAI2 binding peaks relative to the *BIM/BCL2L11* Topologically Associated Domain (TAD). 3D Chromatin interaction via HiChIP for H3K27ac (Red, Top panel) in SMS-CTR cells depicting the TAD containing *BCL2L11* and the SNAI2 peaks within the TAD boundary on the right and near the 3' end of *BIM BCL2L11* on the left (Dark blue, Bottom panel- also shown in figure 6E). Relative position of ChIP-seq tracks

of SNAI2 (Blue), H3K27ac (Yellow) binding at the *BIM/BCL2L11* locus in SMS-CTR cells in shScr cells and delta (Δ) enrichment value (shSNAI2 sh1 minus shScr, Blue and Red) for SNAI2. Boxed area corresponds to SNAI2 binding region and shaded areas represent relative position of the peaks to the TAD and *BCL2L11*. Values on Y-axis represent fold enrichment.

Figure S9

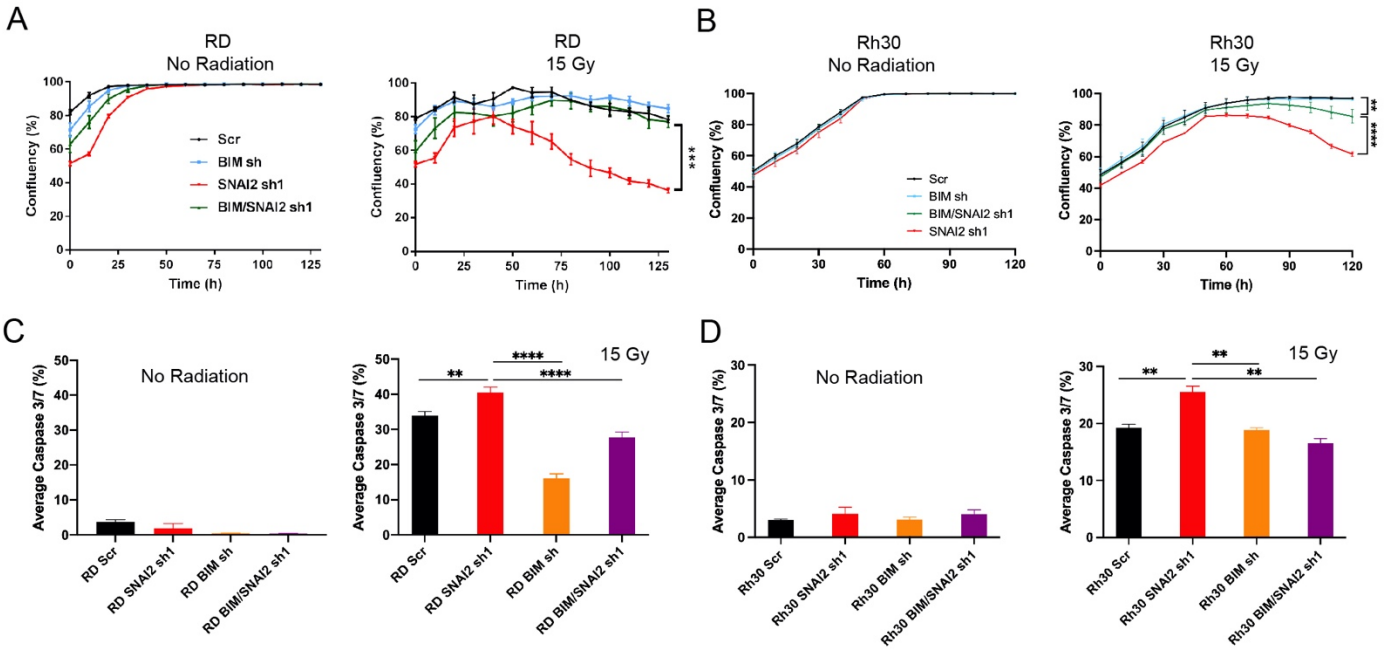

Supplemental Figure 9.

A. Confluency (%) of non-IR or IR (15 Gy) treated RD cells expressing (either control, SNAI2, BIM, or BIM/SNAI2 shRNAs) was assessed using Incucyte Zoom software based on phase-contrast images acquired from 0 h to 125 h. Error bars represent ±1 SD. ***p<0.001 by two-way ANOVA with Sidak's multiple comparisons test.

B. Confluency (%) of non-IR or IR (15 Gy) Rh30 cells (either control, SNAI2, BIM, or BIM/SNAI2 knockdown) was assessed using Incucyte Zoom software based on phase-contrast images acquired from 0 h to 125 h. Error bars represent ±1 SD. **p<0.005, ***p<0.0001 by two-way ANOVA with Sidak's multiple comparisons test.

C. Average Caspase 3/7 (%) (mean ± 1 SD) of RD Scr, SNAI2 sh1, BIM sh, BIM/SNAI2 sh1 cells under non-IR conditions at comparable densities as RD cells 72h after 15 Gy IR. 15 Gy values shown as reference (Figure 6H). No significant difference between cells in non-IR conditions by one-way ANOVA with Tukey's multiple comparisons test.

D. Average Caspase 3/7 (%) (mean ± 1 SD) of Rh30 Scr, SNAI2 sh1, BIM sh, BIM/SNAI2 sh1 cells under non-IR conditions at comparable densities as Rh30 cells 72h after 15 Gy IR. 15 Gy values shown as reference (Figure 6J). No significant differences between cells in non-IR conditions by one-way ANOVA with Tukey's multiple comparisons test.